

# World Journal of *Gastroenterology*

*World J Gastroenterol* 2022 April 14; 28(14): 1384-1502



**EDITORIAL**

- 1384 Hepatocellular adenoma: Where are we now?  
*Wang X, Zhang X*

**OPINION REVIEW**

- 1394 Endoluminal vacuum-assisted therapy to treat rectal anastomotic leakage: A critical analysis  
*Vignali A, De Nardi P*

**REVIEW**

- 1405 Viral hepatitis: Past, present, and future  
*Odenwald MA, Paul S*
- 1430 Osteosarcopenia in autoimmune cholestatic liver diseases: Causes, management, and challenges  
*Pugliese N, Arcari I, Aghemo A, Lania AG, Lleo A, Mazziotti G*

**ORIGINAL ARTICLE****Basic Study**

- 1444 Syngeneic implantation of mouse hepatic progenitor cell-derived three-dimensional liver tissue with dense collagen fibrils  
*Tamai M, Adachi E, Kawase M, Tagawa YI*

**Retrospective Cohort Study**

- 1455 Clinical classification of symptomatic heterotopic pancreas of the stomach and duodenum: A case series and systematic literature review  
*LeCompte MT, Mason B, Robbins KJ, Yano M, Chatterjee D, Fields RC, Strasberg SM, Hawkins WG*

**Retrospective Study**

- 1479 Radiomics signature: A potential biomarker for  $\beta$ -arrestin1 phosphorylation prediction in hepatocellular carcinoma  
*Che F, Xu Q, Li Q, Huang ZX, Yang CW, Wang LY, Wei Y, Shi YJ, Song B*

**LETTER TO THE EDITOR**

- 1494 Comment on review article: Chronic hepatitis C virus infection cascade of care in pediatric patients  
*Bouare N, Keita M, Delwaide J*
- 1499 Comments on "Effect of type 2 diabetes mellitus in the prognosis of acute-on-chronic liver failure patients in China"  
*Wang W, Pan CC, Zhao WY, Sheng JY, Wu QQ, Chen SS*

**ABOUT COVER**

Editorial Board Member of *World Journal of Gastroenterology*, Sung-Chul Lim, MD, PhD, Professor, Head, Department of Pathology, Chosun University Hospital, 365 Pilmun-daero, Dong-gu, Gwangju 61453, South Korea. sclim@chosun.ac.kr

**AIMS AND SCOPE**

The primary aim of *World Journal of Gastroenterology* (WJG, *World J Gastroenterol*) is to provide scholars and readers from various fields of gastroenterology and hepatology with a platform to publish high-quality basic and clinical research articles and communicate their research findings online. WJG mainly publishes articles reporting research results and findings obtained in the field of gastroenterology and hepatology and covering a wide range of topics including gastroenterology, hepatology, gastrointestinal endoscopy, gastrointestinal surgery, gastrointestinal oncology, and pediatric gastroenterology.

**INDEXING/ABSTRACTING**

The WJG is now indexed in Current Contents®/Clinical Medicine, Science Citation Index Expanded (also known as SciSearch®), Journal Citation Reports®, Index Medicus, MEDLINE, PubMed, PubMed Central, and Scopus. The 2021 edition of Journal Citation Report® cites the 2020 impact factor (IF) for WJG as 5.742; Journal Citation Indicator: 0.79; IF without journal self cites: 5.590; 5-year IF: 5.044; Ranking: 28 among 92 journals in gastroenterology and hepatology; and Quartile category: Q2. The WJG’s CiteScore for 2020 is 6.9 and Scopus CiteScore rank 2020: Gastroenterology is 19/136.

**RESPONSIBLE EDITORS FOR THIS ISSUE**

Production Editor: *Hua-Ge Yan*, Production Department Director: *Xu Guo*, Editorial Office Director: *Ze-Mao Gong*.

**NAME OF JOURNAL**

*World Journal of Gastroenterology*

**ISSN**

ISSN 1007-9327 (print) ISSN 2219-2840 (online)

**LAUNCH DATE**

October 1, 1995

**FREQUENCY**

Weekly

**EDITORS-IN-CHIEF**

Andrzej S Tarnawski

**EDITORIAL BOARD MEMBERS**

<http://www.wjgnet.com/1007-9327/editorialboard.htm>

**PUBLICATION DATE**

April 14, 2022

**COPYRIGHT**

© 2022 Baishideng Publishing Group Inc

**INSTRUCTIONS TO AUTHORS**

<https://www.wjgnet.com/bpg/gerinfo/204>

**GUIDELINES FOR ETHICS DOCUMENTS**

<https://www.wjgnet.com/bpg/GerInfo/287>

**GUIDELINES FOR NON-NATIVE SPEAKERS OF ENGLISH**

<https://www.wjgnet.com/bpg/gerinfo/240>

**PUBLICATION ETHICS**

<https://www.wjgnet.com/bpg/GerInfo/288>

**PUBLICATION MISCONDUCT**

<https://www.wjgnet.com/bpg/gerinfo/208>

**ARTICLE PROCESSING CHARGE**

<https://www.wjgnet.com/bpg/gerinfo/242>

**STEPS FOR SUBMITTING MANUSCRIPTS**

<https://www.wjgnet.com/bpg/GerInfo/239>

**ONLINE SUBMISSION**

<https://www.f6publishing.com>

## Retrospective Study

Radiomics signature: A potential biomarker for  $\beta$ -arrestin1 phosphorylation prediction in hepatocellular carcinoma

Feng Che, Qing Xu, Qian Li, Zi-Xing Huang, Cai-Wei Yang, Li Ye Wang, Yi Wei, Yu-Jun Shi, Bin Song

**Specialty type:** Gastroenterology and hepatology**Provenance and peer review:** Invited article; Externally peer reviewed.**Peer-review model:** Single blind**Peer-review report's scientific quality classification**Grade A (Excellent): A  
Grade B (Very good): 0  
Grade C (Good): C  
Grade D (Fair): 0  
Grade E (Poor): 0**P-Reviewer:** Costa G, Italy; Gumbs A, France**Received:** November 9, 2021**Peer-review started:** November 9, 2021**First decision:** January 9, 2022**Revised:** January 22, 2022**Accepted:** March 6, 2022**Article in press:** March 6, 2022**Published online:** April 14, 2022**Feng Che, Qian Li, Zi-Xing Huang, Cai-Wei Yang, Yi Wei, Bin Song**, Department of Radiology, West China Hospital, Sichuan University, Chengdu 610041, Sichuan Province, China**Qing Xu, Yu-Jun Shi**, Institute of Clinical Pathology, West China Hospital, Sichuan University, Chengdu 610041, Sichuan Province, China**Li Ye Wang**, Department of Research and Development, Shanghai United Imaging Intelligence Co., Ltd, Shanghai 200232, China**Corresponding author:** Bin Song, MD, Chief Doctor, Doctor, Professor, Department of Radiology, West China Hospital, Sichuan University, No 37, Guoxue Alley, Wuhou District, Chengdu 610041, Sichuan Province, China. [songlab\\_radiology@163.com](mailto:songlab_radiology@163.com)**Abstract****BACKGROUND**

The phosphorylation status of  $\beta$ -arrestin1 influences its function as a signal strongly related to sorafenib resistance. This retrospective study aimed to develop and validate radiomics-based models for predicting  $\beta$ -arrestin1 phosphorylation in hepatocellular carcinoma (HCC) using whole-lesion radiomics and visual imaging features on preoperative contrast-enhanced computed tomography (CT) images.

**AIM**

To develop and validate radiomics-based models for predicting  $\beta$ -arrestin1 phosphorylation in HCC using radiomics with contrast-enhanced CT.

**METHODS**

Ninety-nine HCC patients (training cohort:  $n = 69$ ; validation cohort:  $n = 30$ ) receiving systemic sorafenib treatment after surgery were enrolled in this retrospective study. Three-dimensional whole-lesion regions of interest were manually delineated along the tumor margins on portal venous CT images. Radiomics features were generated and selected to build a radiomics score using logistic regression analysis. Imaging features were evaluated by two radiologists independently. All these features were combined to establish clinico-radiological (CR) and clinico-radiological-radiomics (CRR) models by using multivariable logistic regression analysis. The diagnostic performance and clinical usefulness of the models were measured by receiver operating characteristic and decision curves, and the area under the curve (AUC) was determined. Their association

with prognosis was evaluated using the Kaplan-Meier method.

## RESULTS

Four radiomics features were selected to construct the radiomics score. In the multivariate analysis, alanine aminotransferase level, tumor size and tumor margin on portal venous phase images were found to be significant independent factors for predicting  $\beta$ -arrestin1 phosphorylation-positive HCC and were included in the CR model. The CRR model integrating the radiomics score with clinico-radiological risk factors showed better discriminative performance (AUC = 0.898, 95%CI, 0.820 to 0.977) than the CR model (AUC = 0.794, 95%CI, 0.686 to 0.901;  $P = 0.011$ ), with increased clinical usefulness confirmed in both the training and validation cohorts using decision curve analysis. The risk of  $\beta$ -arrestin1 phosphorylation predicted by the CRR model was significantly associated with overall survival in the training and validation cohorts (log-rank test,  $P < 0.05$ ).

## CONCLUSION

The radiomics signature is a reliable tool for evaluating  $\beta$ -arrestin1 phosphorylation which has prognostic significance for HCC patients, providing the potential to better identify patients who would benefit from sorafenib treatment.

**Key Words:** Hepatocellular carcinoma; Sorafenib resistance;  $\beta$ -Arrestin1 phosphorylation; Radiomics; Computed tomography; Overall survival

©The Author(s) 2022. Published by Baishideng Publishing Group Inc. All rights reserved.

**Core Tip:** The aim of this study was to develop and validate radiomics-based models for predicting  $\beta$ -arrestin1 phosphorylation in hepatocellular carcinoma (HCC). A total of 99 HCC patients (training cohort:  $n = 69$ ; validation cohort:  $n = 30$ ) were included, and the final clinico-radiological-radiomics model integrating the radiomics scores and clinico-radiological risk factors showed satisfactory discriminative performance (AUC = 0.898, 95%CI, 0.820 to 0.977). The preoperative prediction model can be used as a noninvasive and effective tool to help predict the outcome of HCC patients treated with sorafenib and identify patients who would benefit most from sorafenib treatment.

**Citation:** Che F, Xu Q, Li Q, Huang ZX, Yang CW, Wang LY, Wei Y, Shi YJ, Song B. Radiomics signature: A potential biomarker for  $\beta$ -arrestin1 phosphorylation prediction in hepatocellular carcinoma. *World J Gastroenterol* 2022; 28(14): 1479-1493

**URL:** <https://www.wjgnet.com/1007-9327/full/v28/i14/1479.htm>

**DOI:** <https://dx.doi.org/10.3748/wjg.v28.i14.1479>

## INTRODUCTION

Hepatocellular carcinoma (HCC) was the sixth most common cancer and the third leading cause of cancer-related death worldwide in 2020[1]. Liver resection and transplantation are considered potentially curative methods for early-stage patients with well-preserved liver function. For advanced-stage HCC, systemic therapies such as multikinase inhibitors and immune checkpoint inhibitors, represented by sorafenib, have shown the potential to confer a survival advantage of 2-3 mo[2,3]. However, patients undergoing sorafenib treatment have a high resistance rate, which is still the greatest challenge and leads to a discouraging prognosis[3]. Hence, identifying patients who are more likely to benefit from sorafenib treatment and discovering related biomarkers associated with sorafenib treatment response are urgently needed.

$\beta$ -Arrestins, including  $\beta$ -arrestin1 and  $\beta$ -arrestin2, are important regulators of seven-transmembrane domain G-protein-coupled receptors. They can block subsequent G protein activation and result in receptor desensitization by phosphorylation/dephosphorylation of  $\beta$ -arrestin1 at a carboxyl-terminal serine, Ser-412[4,5]. The development of sorafenib resistance includes primary and secondary resistance, and the phosphorylation of ERK has been widely accepted to play an important role in both[6-8]. Activation of AKT and epithelial-mesenchymal transition (EMT) also participates in acquired resistance and the signaling pathways mentioned above have strong relationships with  $\beta$ -arrestin1[9-11]. Wu *et al* revealed that  $\beta$ -arrestin1 enhances hepatocellular carcinogenesis by inflammation-mediated Akt signaling[12] and promotes HCC invasion and metastasis through p-ERK1/2 to mediate EMT[13]. The phosphorylation status of  $\beta$ -arrestin1 influences its function in activating downstream receptors such as

ERK1/2, forming a negative feedback loop[14]. All these signals are highly related to sorafenib resistance[9,15], which indicates that the expression of phosphorylated  $\beta$ -arrestin1 (p- $\beta$ -arrestin1) may correlate with sorafenib resistance in HCC patients. Thus, the preoperative prediction of  $\beta$ -arrestin1 phosphorylation may help identify patients who could benefit from sorafenib treatment.

Radiomics is a newly emerging computational medical imaging method that allows for the quantitative analysis and translation of medical images[16,17]. Additionally, radiomics studies can provide insights into the depth and comprehensive characterization of tumor heterogeneity, with the underlying hypothesis that radiomics can better characterize tumor heterogeneity[18-20]. Preliminary studies have suggested that radiomics features can be useful for tumor lesion detection[18,21] and are potentially predictive of the microenvironment and molecular status of tumors[16,22,23]. Xu *et al*[24] extracted radiomics signatures from contrast-enhanced computed tomography (CECT) images to build a risk model that showed good performance in microvascular invasion stratification and could well predict the clinical outcomes of HCC patients. To the best of our knowledge, the value of radiomics based on CECT images in predicting  $\beta$ -arrestin1 phosphorylation in HCC has not yet been reported.

The purpose of this study was therefore to develop and validate a radiomics-based model combining visual imaging and clinical features for the preoperative noninvasive prediction of  $\beta$ -arrestin1 phosphorylation and to further investigate its association with prognostic outcomes in HCC patients.

## MATERIALS AND METHODS

### Patients

This retrospective study was approved by the Institutional Review Board of West China Hospital and the requirement for informed consent was waived. Patients who had histologically proven HCC and received systemic treatment with sorafenib after surgery between January 2013 and April 2017 were retrospectively reviewed and consecutively recorded. The inclusion criteria were as follows: (1) Age  $\geq 18$  years; (2) Pathologically confirmed HCC; (3) Interval between CECT imaging and surgery less than four weeks; (4) Treatment naive [*i.e.*, no hepatectomy, transcatheter arterial chemoembolization (TACE) or radiofrequency ablation (RFA) before CECT]; and (5) Administration of 400 mg sorafenib twice a day after surgery with up to two dose reductions allowed (from 400 mg once daily to 400 mg every 2 d) for drug-related adverse events. The exclusion criteria were as follows: (1) Incomplete or poor-quality CT images; (2) Interrupted sorafenib treatment for longer than 48 h between the initiation of sorafenib and the first follow-up time point; and (3) Death or loss to follow-up. Among the 146 eligible patients, 47 patients were excluded because CECT imaging was performed more than 4 wk before surgery ( $n = 13$ ), the CT images were incomplete or of poor quality ( $n = 11$ ), sorafenib treatment was interrupted for longer than 48 h between the initiation of sorafenib and the first follow-up time point ( $n = 8$ ), or the patient was lost to follow-up ( $n = 15$ ). Therefore, 99 patients were ultimately enrolled in this study. In addition, the investigated laboratory data within 7 days of the CT examination and clinical conditions were recorded, as shown in Figure 1.

In this study, consecutive patients who underwent surgery between January 2013 and March 2016 comprised the training cohort and were used to construct the nomograms, and patients who underwent surgery from April 2016 to April 2017 comprised the validation cohort.

### Imaging techniques

CT imaging was performed by using multidetector CT scanners (Revolution, GE Healthcare, Milwaukee, United States; SOMATOM definition, Siemens Healthcare, Erlangen, Germany). Precontrast images were first obtained before contrast agent (iodine concentration, 300-370 mg/mL; volume, 1.5-2.0 mL/kg of body weight; contrast type, iopromide injection, Bayer Pharma AG) injection. Then, the arterial phase and portal venous phase were obtained with the following parameters: tube voltage, 100-120 kVp; tube current, 450 mA; slice thickness, 0.625 mm; pitch, 0.992:1; rotation speed: 0.5 s/rot; and ASIR-V: 30%. The arterial phase and portal venous phase were obtained at 25 s and 60 s after contrast injection.

### Imaging evaluation

Three abdominal radiologists who were blinded to the histopathological results, clinical data, and survival outcomes reviewed all the CT images. The following imaging features were assessed by these readers: (1) Tumor margin, defined as a non-smooth margin with budding portion protruding into the liver parenchyma or infiltrative appearance at the tumor periphery, otherwise as smooth margin; (2) Tumor size, defined as the maximum diameter, measured on arterial phase transverse images or portal venous phase images; (3) Pseudocapsule, defined as a complete capsule with a uniform border around most or all of the tumor, unequivocally thicker or more conspicuous than the fibrotic tissue around background nodules, otherwise as incomplete integrity or not applicable; (4) Multifocality; (5) Arterial phase hyperenhancement; (6) Portal venous/delay phase hypoenhancement; (7) Radiologic evidence of necrosis; (8) Radiologic evidence of cirrhosis; and (9) Portal vein tumor thrombosis invasion. All examinations were performed using a workstation and recorded on a picture archiving and

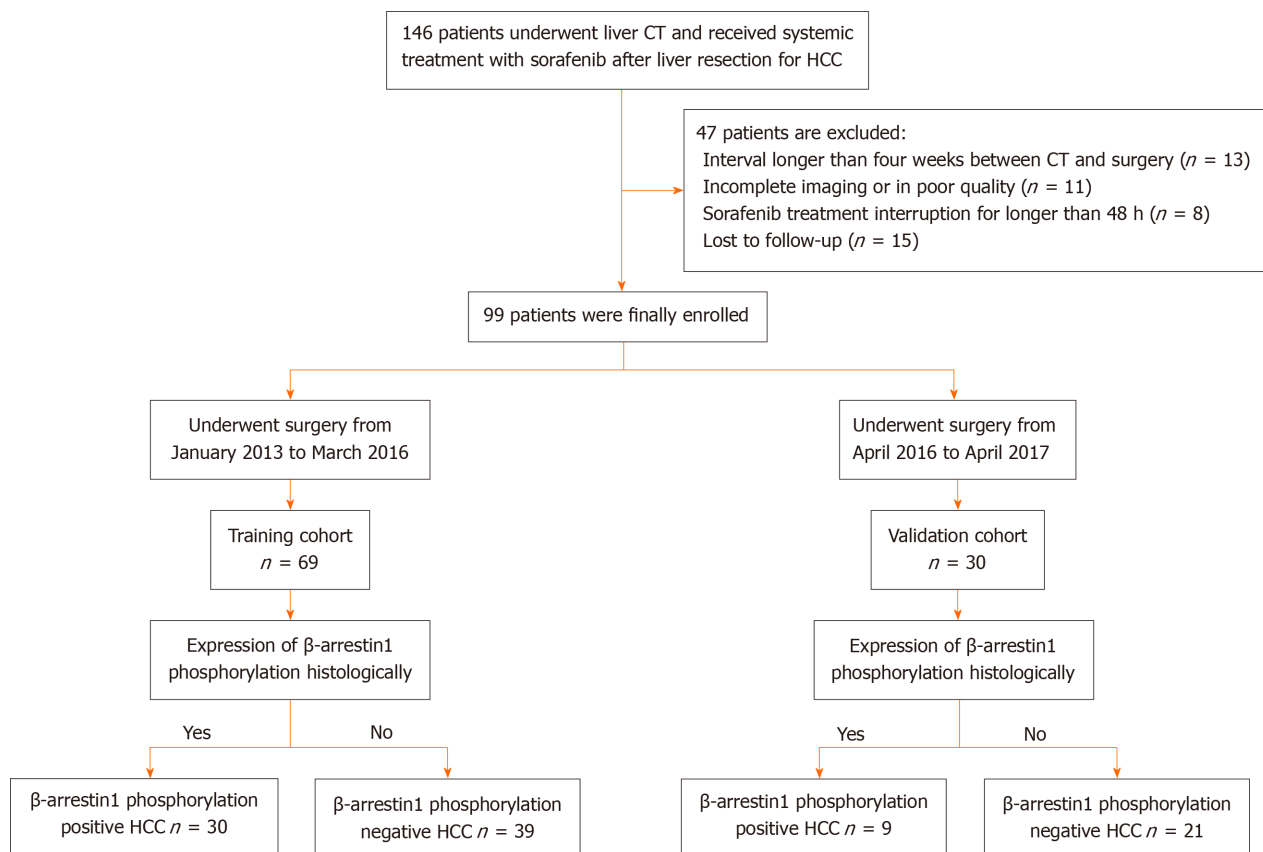


Figure 1 Patient recruitment process.

communication system.

### Immunohistochemistry

Surgically resected specimens embedded in paraffin were cut into 4  $\mu$ m-thick sections dewaxed, hydrated, and subjected to antigen retrieval. Subsequently, the tissue slides were incubated with primary antibodies using rabbit anti-human p- $\beta$ -arrestin1 polyclonal antibody (Abcam Biotechnology, ab247229; diluted, 1:200) at 4 °C overnight, followed by incubation with secondary antibodies (cat # K5007; Dako). Staining was performed with 3,3'-diaminobenzidine (DAB) and counterstained with hematoxylin. Two senior pathologists who were blinded to all radiological and clinical results independently selected five nonoverlapping and discontinuous regions to calculate the mean for statistical analysis. Variations in the results within a range of 5% were reassessed, and a consensus decision was made. With the threshold value of 5% (p- $\beta$ -arrestin1 tumor cells/total tumor cells), cases with expression higher than 5% were considered p- $\beta$ -arrestin1 positive.

### Follow-up surveillance after surgical resection

The patients were consistently followed-up after liver resection at intervals of 3 to 6 mo based on  $\alpha$ -fetoprotein and imaging examinations, including ultrasound, CT or magnetic resonance imaging (MRI), and the time of disease-specific progression (local recurrence or distant organ metastasis) and time of death were recorded. These survival data were collected by one radiologist using electronic medical records and follow-up imaging studies until June 30, 2020. Overall survival (OS) was measured as the interval from the date of surgery to the date of death from a disease-related cause or the latest follow-up. For patients who were alive at the latest follow-up, the data were censored.

### Radiomics workflow

Regions of interest (ROIs) were manually delineated around the outline of the tumor slice by slice using ITK-SNAP software (version 3.6.0) and excluded necrosis and calcification in the tumors. Radiomics features were generated from the images using in-house scientific research 3D analysis software (Analysis Kit, version V3.0.0. R, GE healthcare). Two classes of feature extraction methods were extracted as follows: the original feature class and 14 filter classes (boxmean, additiveGaussiannoise, binomialblurimage, curvatureflow, boxsigmainage, log, wavelet, normalize, laplaciansharpening, discreteGaussian, mean, specklenoise, recursiveGaussian and shotnoise). A total of 2600 features were extracted from the tumors. Two radiologists (readers 1 and 2) performed ROI segmentation in a blinded

manner to assess interobserver reliability. Reader 1 repeated the feature extraction twice during a 1-wk period to evaluate intraobserver reliability. The interobserver reliability and intraobserver reliability were assessed by obtaining the intraclass correlation coefficient (ICC). Features with ICC values  $> 0.75$  were selected for subsequent investigation. The feature selection process comprised the following three steps in the training group: variance analysis, Spearman correlation, and Lasso regression analysis. The radiomics score of each patient was calculated using this determined multivariable logistic regression model.

### **Prediction models of $\beta$ -arrestin1 phosphorylation**

For CT radiographic and clinical factors, predictors with  $P < 0.05$  in the univariate logistic analysis ( $P < 0.05$ ) were included. Multivariate logistic analysis, which was used to identify significant predictors based on a backward stepwise selection process with the Akaike information criterion, was employed to develop a clinical-radiological (CR) model. In addition, a clinical-radiological-radiomics (CRR) model was constructed by multivariate logistic regression analysis, tests of the association with radiomics scores, clinical factor evaluations and CT imaging findings based on a backward stepwise selection process with the Akaike information criterion.

### **Statistical analysis**

Categorical variables are summarized as frequencies and proportions, while continuous variables are expressed as the means and standard deviations or medians and interquartile ranges (IQRs). The differences in characteristics between groups were evaluated using Student's *t* test (normal distribution) and the Mann-Whitney *U* test (skewed distribution) for continuous variables and the chi-squared test or Fisher's exact test for categorical variables. OS curves were drawn by using the Kaplan-Meier method, and the difference in OS between groups was compared using the log-rank test. Inter-observer agreement was applied to assess the reliability of imaging analysis using the Kappa test; 0-0.2 represents slight, 0.21-0.40: fair, 0.41-0.60: moderate, 0.61-0.80: substantial, 0.81-1: excellent.

The discriminative performance of the prediction models was quantified by the area under the curve (AUC) of receiver operator characteristic (ROC) curves. Differences in the ROC curves were compared by using the DeLong test. Calibration curves were generated to assess the calibration of the prediction model with the Hosmer-Lemeshow test. The probabilities of net benefits were quantified by decision curve analysis to evaluate the clinical application value of the prediction models.

The statistical analyses were implemented using *R* statistical software (version 3.4.2, <http://www.R-project.org>) and SPSS software (version 22.0, IBM), and two-sided *P* values  $< 0.05$  were considered significant.

## **RESULTS**

### **Patient characteristics**

Of the 99 patients [male/female: 88/11; mean age,  $51.53 \pm 12.62$  years, range 21 to 78 years) included in the study (training ( $n = 69$ ) and validation ( $n = 30$ ]), p- $\beta$ -arrestin1 was identified in 39 (39.4%) patients. The 3-year survival rates of p- $\beta$ -arrestin1-positive and p- $\beta$ -arrestin1-negative HCC patients were 38.5% and 31.7%, respectively. The Kaplan-Meier method showed that p- $\beta$ -arrestin1-positive patients lived longer than p- $\beta$ -arrestin1-negative patients ( $P < 0.05$  with the log-rank test). The clinical, pathological, and imaging characteristics of patients in the training and validation cohorts are summarized in [Table 1](#).

### **Development of the radiomics score**

Variance analysis using *t* test identified 15 radiomics features, assessed by Spearman rank correlation, and 4 features (boxsigmainage\_glrmlm\_RunLengthNonUniformity, wavelet\_firstorder\_wavelet-HLL-Skewness, wavelet\_glcm\_wavelet-HLH-Correlation, and wavelet\_ngtdm\_wavelet-LHL-Busyness) were chosen for logistic regression analysis ( $P > 0.05$ ). Variables with  $P < 0.1$  in the univariable logistic regression analysis were included in the multivariable regression model with backward stepwise selection using the Akaike information criterion. The radiomics score was calculated with the following formula: radiomics score =  $-0.3527 + 0.4748 \times \text{boxsigmainage\_glrmlm\_RunLengthNonUniformity} + 0.7046 \times \text{wavelet\_firstorder\_wavelet-HLL-Skewness} - 0.5697 \times \text{wavelet\_glcm\_wavelet-HLH-Correlation} + 0.6471 \times \text{wavelet\_ngtdm\_wavelet-LHL-Busyness}$ .

### **Development of the predictive models**

In total, 2 clinical characteristics [alanine aminotransferase (ALT) and aspartate aminotransferase (AST) levels], 2 imaging features (tumor size and tumor margin on portal venous phase images) and the radiomics score were identified by univariate analysis (all  $P < 0.1$ ). In the multivariable logistic regression analysis, radiomics score [odds ratio (OR), 3.412; 95%CI: 1.562-7.453,  $P = 0.002$ ], ALT level (OR, 0.159; 95%CI: 0.038-0.673,  $P < 0.012$ ), tumor size (OR, 0.243; 95%CI: 0.059-1.003,  $P = 0.05$ ) and tumor margin (OR, 0.170; 95%CI: 0.044-0.664,  $P = 0.011$ ) significantly predicted  $\beta$ -arrestin1 phosphorylation

**Table 1** Baseline characteristics of the patients in the training and validation cohorts

Variables	Training cohort (n = 69)	Validation cohort (n = 30)	P value
Age, mean $\pm$ SD, yr	51.00 $\pm$ 13.019	52.73 $\pm$ 11.776	0.269
Gender			0.751
Male	61 (88.4)	26 (86.7)	
ALT (IU/L)			0.375
< 40	44 (63.8)	16 (53.5)	
AST (IU/L)			0.829
< 35	32 (46.4)	13 (43.4)	
ALB (g/L)			0.612
< 40	15 (21.7)	8 (26.7)	
GGT ( $\mu$ /L)			0.817
< 45	24 (34.8)	9 (30.0)	
TBIL ( $\mu$ mol/L)			0.828
< 17.1	39 (56.5)	16 (53.3)	
PLT ( $\times 10^9$ /L)			0.791
< 100	14 (20.3)	7 (23.3)	
PT(s)			0.596
< 9.6 or > 12.8	16 (23.2)	5 (16.7)	
AFP (ng/mL)			0.279
< 400	34 (49.3)	11 (36.7)	
CEA (ng/mL)			0.798
< 3.4	53 (76.8)	24 (80.0)	
HBsAg			0.270
Positive	61 (88.4)	29 (96.7)	
MVI			0.827
Absent	36 (52.2)	17 (56.7)	
Present	33 (47.8)	13 (43.3)	
Differentiation			0.661
Highly	37 (53.6)	18 (60.0)	
Middle-Low	32 (46.4)	12 (40.0)	
BCLC			0.254
0-A	9 (13.0)	8 (26.7)	
B	28 (40.6)	10 (33.3)	
C	32 (46.4)	12 (40.0)	
Child-Pugh Score			0.770
< 3	57 (82.6)	26 (86.7)	
Morphologic CT features			
Tumour size			0.499
< 5 cm	24 (34.8)	13 (43.3)	
Multifocality			0.351
1	49 (71.0)	18 (60.0)	
$\geq 2$	20 (29.0)	12 (40.0)	

Tumour margin			0.661
Smooth	32 (46.4)	12 (40.0)	
Non-smooth	37 (53.6)	18 (60.0)	
Pseudo-capsule			0.824
Well-defined	27 (39.1)	13 (43.3)	
Ill-defined	42 (60.9)	17 (56.7)	
AP hyperenhancement			0.448
No	5 (7.2)	4 (13.3)	
Yes	64 (92.8)	26 (86.7)	
PVP hypoenhancement			0.430
No	4 (5.8)	3 (10.0)	
Yes	65 (94.2)	27 (90.0)	
Radiologic evidence of necrosis			0.822
Absent	25 (36.2)	12 (40.0)	
Present	44 (63.8)	18 (60.0)	
Radiologic evidence of cirrhosis			0.654
Absent	45 (65.2)	18 (60.0)	
Present	24 (34.8)	12 (40.0)	
Portal vein tumor thrombosis invasion			0.186
Absent	43 (62.3)	14 (46.7)	
Present	26 (37.7)	16 (53.3)	

Note: Unless otherwise indicated, data are the number of patients, and data in parentheses are percentages. AFP: Alpha-fetoprotein; CEA: Carcinoembryonic antigen; HBsAg: Hepatitis B surface antigen; ALT: Alanine aminotransferase; AST: Aspartate aminotransferase; TBIL: Total bilirubin; ALB: Albumin; PT: Prothrombin time; PLT: Platelet count; GGT:  $\gamma$ -glutamyl transpeptidase; MVI: Microvascular invasion; BCLC: Barcelona Clinic Liver Cancer; SD: Standard deviation; AP: Arterial phase; PVP: Portal venous phase.

(Table 2). Thus, the CR and CRR models were constructed by using the above aggressive features and the nomograms of the above multiparametric models are shown in Figure 2A and B. Excellent interobserver agreement was observed for the imaging feature evaluation, with Kappa values of 0.890 for tumor size and 0.789 for smooth tumor margin (Figure 3).

### Predictive performance of the models

In the training cohort, the AUCs of the radiomics score, CR model and CRR model were 0.754 (95%CI: 0.640-0.868), 0.794 (95%CI: 0.686-0.901) and 0.898 (95%CI: 0.820-0.977), respectively. The CRR model had a significantly higher AUC than the radiomics score ( $P = 0.007$ ) and the CR model ( $P = 0.011$ ). In the validation cohort, the AUCs of the radiomics score, CR model and CRR model were 0.704 (95%CI: 0.454-0.953), 0.646 (95%CI: 0.411-0.880) and 0.735 (95%CI: 0.505-0.966), respectively. The diagnostic performance of the radiomics score and two models is shown in Table 3 and Figure 2C and D. The calibration curve of all the models showed excellent agreement between the predictions and observations in both the training and validation cohorts (all  $P > 0.05$ ) (Figure 2E and F). The decision curve showed that the CRR model had the largest overall net benefit compared with the treat-all-patients as p- $\beta$ -arrestin1 positive and treat-none patients as p- $\beta$ -arrestin1 negative across the full range of reasonable threshold probabilities (Figure 4).

### Risk stratification with p- $\beta$ -arrestin1 predicted by the CRR model

According to the risk of  $\beta$ -arrestin1 phosphorylation predicted by the CRR model, patients with p- $\beta$ -arrestin1 positivity lived longer than those with p- $\beta$ -arrestin1 negativity using the log-rank test ( $P < 0.05$ ) in both the training and validation cohorts (Figure 5).

**Table 2 Univariate and multivariate regression analyses of the p- $\beta$ -arrestin1-positive and p- $\beta$ -arrestin1-negative groups in the training cohort**

Variables	Univariable analysis		Multivariable analysis	
	OR (95%CI)	P value	OR (95%CI)	P value
ALT	0.237 (0.043-1.292)	0.096 <sup>a</sup>	0.159 (0.038-0.673)	0.012 <sup>a</sup>
AST	0.497 (0.100-2.471)	0.393	-	-
Tumor size	0.245 (0.059-1.019)	0.053 <sup>a</sup>	0.243 (0.059-1.003)	0.050 <sup>a</sup>
Tumor margin	0.180 (0.046-0.706)	0.014 <sup>a</sup>	0.170 (0.044-0.664)	0.011 <sup>a</sup>
Radiomics	3.473 (1.574-7.663)	0.002 <sup>a</sup>	3.412 (1.562-7.453)	0.002 <sup>a</sup>

<sup>a</sup>P value < 0.1.

ALT: Alanine aminotransferase; AST: Aspartate aminotransferase; CI: Confidence interval; OR: Odds ratio.

**Table 3 Diagnostic performance of the three models for predicting  $\beta$ -arrestin1 phosphorylation-positive hepatocellular carcinoma**

	Training group				Validation cohort			
	AUC (95%CI)	SPE	SEN	P value	AUC (95%CI)	SPE	SEN	P value
RS	0.754 (0.640-0.868)	53.8	86.7	0.007 <sup>1</sup>	0.704 (0.454-0.953)	47.6	77.8	0.791 <sup>1</sup>
CR	0.794 (0.686-0.901)	87.2	66.7	0.631 <sup>2</sup>	0.646 (0.411-0.880)	81.0	33.3	0.713 <sup>2</sup>
CRR	0.898 (0.820-0.977)	87.2	86.7	0.011 <sup>3</sup>	0.735 (0.505-0.966)	71.4	66.7	0.147 <sup>3</sup>

<sup>1</sup>AUCs of the radiomics score and clinico-radiological-radiomics model were compared.

<sup>2</sup>AUCs of the radiomics score and clinico-radiological model were compared.

<sup>3</sup>AUCs of the clinico-radiological model and clinico-radiological-radiomics model were compared.

RS: Radiomics score; CR: Clinico-radiological; CRR: Clinico-radiological-radiomics; SEN: Sensitivity; SPE: Specificity; AUC: Area under the curve; CI: Confidence interval.

## DISCUSSION

In this retrospective study, a CT image-based model incorporating qualitative imaging features, clinical characteristics and quantitative radiomics features for predicting  $\beta$ -arrestin1 phosphorylation in HCC was generated. In addition, in patients treated with sorafenib, we found that p- $\beta$ -arrestin1-positive HCC patients predicted by the CRR model were associated with better prognosis. The CRR model may serve as a noninvasive and effective tool to predict HCC patients  $\beta$ -arrestin1 phosphorylation status and help select patients who are suitable for sorafenib treatment.

For predicting  $\beta$ -arrestin1 phosphorylation in HCC patients, radiomics features provided increased power (AUC = 0.754) and were indicated to be independent predictors for p- $\beta$ -arrestin1 in the final CRR model ( $P = 0.005$ ). Utilizing the radiomics method, the proposed CRR model yielded an improved diagnostic performance in the training cohort (AUC from 0.794 to 0.898) and validation cohort (AUC from 0.646 to 0.735), indicating that the combined radiomics approach may have greater value in preoperative  $\beta$ -arrestin1 phosphorylation prediction than clinico-radiological features. The reason why the CRR model achieved the best predictive performance can be explained by the fact that the final model includes both qualitative and quantitative imaging features to provide a comprehensive overview of the correlations of radiomics features with HCC pathological status and genomics characteristics[25]. The radiomics signature includes shape, intensity, and texture information, which can reflect the complexity of the properties of the target tissue. Previous studies have shown that imaging features, including texture features, are informative of the gene expression profiles of HCC lesions, which parallels the diversity of molecular activities[26]. Hectors *et al* found that MRI radiomics features are highly associated with HCC immuno-oncological characteristics and can serve as noninvasive predictors of its status[27]. A predictive nomogram incorporating a radiomics signature and other clinico-radiological factors showed a significantly improved diagnostic performance in cytokeratin19 stratification of HCC[28]. However, to our knowledge, no other studies have investigated the possible value of quantitative analysis integrating clinical factors in predicting  $\beta$ -arrestin1 phosphorylation in HCC. Developed in the training cohort and applied to the validation cohort, the radiomics score based on CECT images combined with clinico-radiological factors could correctly identify the  $\beta$ -arrestin1 phosphorylation status of more than 86.7% of the patients in the training cohort and was well validated

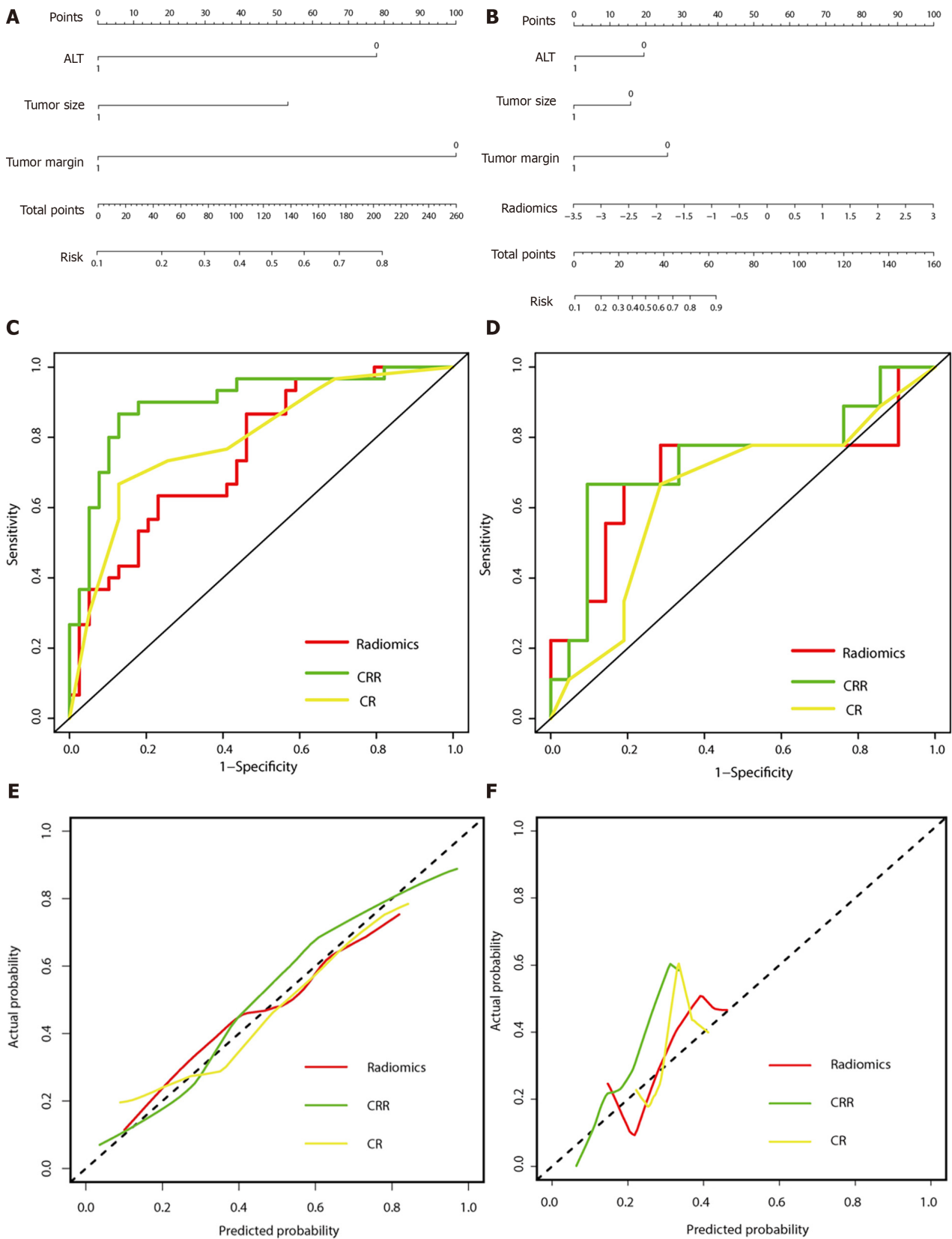


**Figure 2 Performance of the three models.** A: The developed clinico-radiological (CR) nomogram; B: The developed clinico-radiological-radiomics (CRR) nomogram. Predictor points are found on the uppermost point scale that corresponds to each variable. On the bottom scale, the points for all variables are added and translated into a  $\beta$ -arrestin1 phosphorylation positivity probability. C: Comparison of receiver operating characteristic (ROC) curves of the radiomics model, CR model and CRR model in the training cohort; D: Comparison of receiver operating characteristic (ROC) curves of the radiomics model, CR model and CRR model in the validation cohort. E: Calibration curves of the three models in the training cohort; F: Calibration curves of the three models in the validation cohort. The actual high expression of p- $\beta$ -arrestin1 is represented on the y-axis, and the predicted probability is represented on the x-axis. The closer fit of the solid line to the ideal black dotted line indicates a better calibration.

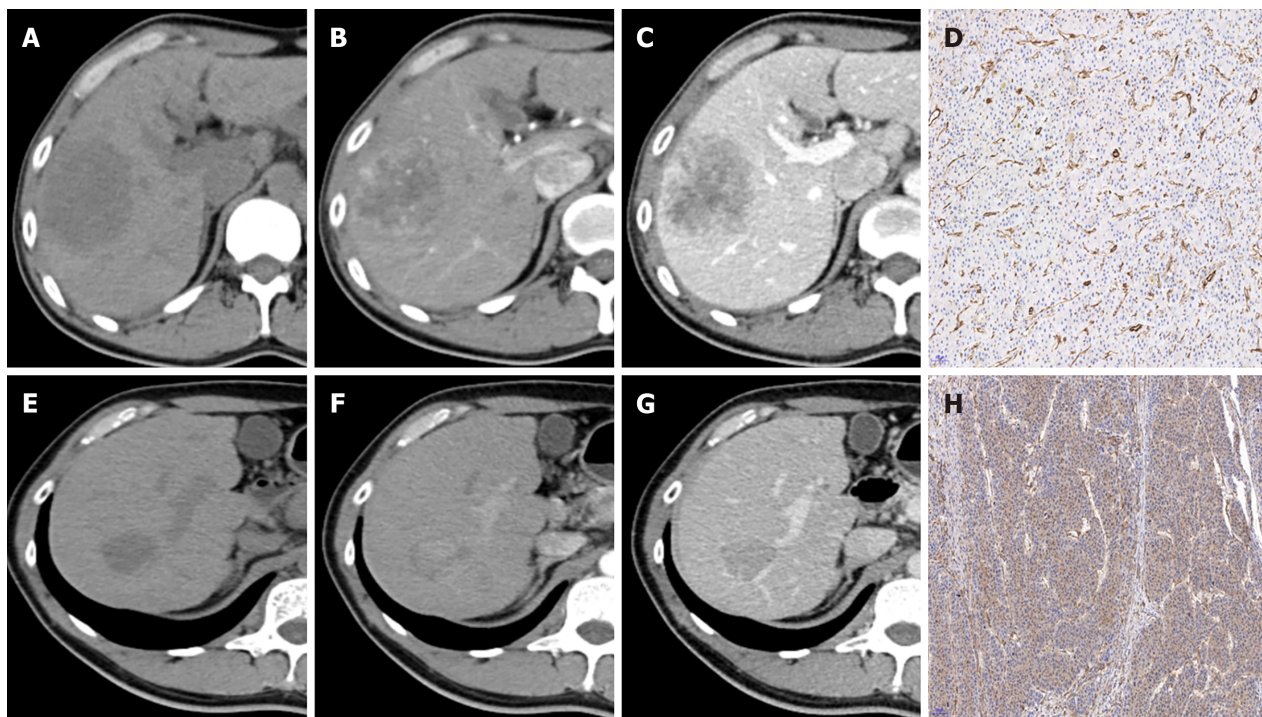


**Figure 3 Representative images of contrast-enhanced computed tomography and  $\beta$ -Arrestin1 phosphorylation (magnification,  $\times 100$ ).** A: CT images of a 45-year-old man with a 6.3-cm hepatocellular carcinoma (HCC) in the right liver lobe in the plain phase; B: The tumor shows heterogeneous hyperenhancement in the arterial phase; C: The tumor shows washout at the portal venous phase with intratumor necrosis, an ill-defined capsule and a non-smooth tumor margin. D: Immunohistochemical staining shows a  $\beta$ -arrestin1 phosphorylation-negative status at 100 $\times$  magnification.

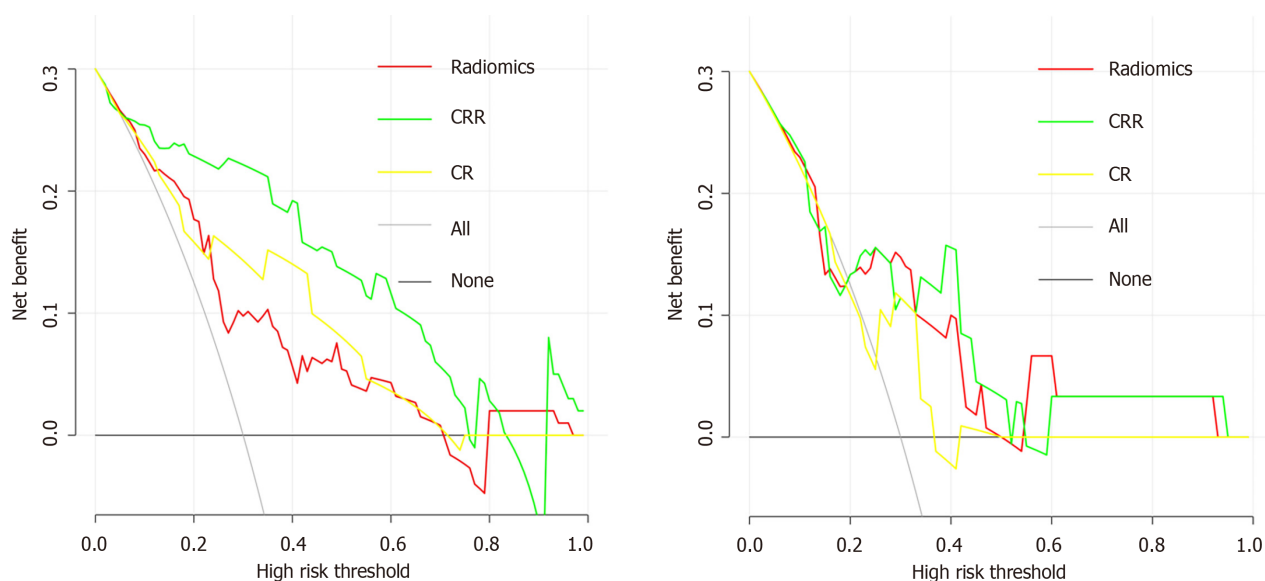


**Figure 4 Decision curve analysis for each model.** A: Decision curve analysis in the training cohort; B: Decision curve analysis in the validation cohort. The y-axis measures the net benefit, and the x-axis is the threshold probability. The gray line represents the hypothesis that all patients are  $\beta$ -arrestin1 phosphorylation-positive. The black line represents the hypothesis that all patients are  $\beta$ -arrestin1 phosphorylation-negative. Among the three models, the clinico-radiological-radiomics (CRR) model provided the highest net benefit compared with the radiomics and clinico-radiological (CR) models.

to serve as a quantitative multiple-feature parameter for the  $\beta$ -arrestin1 phosphorylation-based risk stratification of HCC patients. Our study investigates the predictive aspects of computational-assisted models for the preoperative prediction of  $\beta$ -arrestin1 phosphorylation status, which currently can now only be attained by invasive biopsy or surgery. This computational method can guide clinical management by identifying patients for targeted therapy, as most patients recommended for systematic treatment according to the Barcelona Clinic Liver Cancer algorithm are not candidates for surgery due to their poor condition[29].

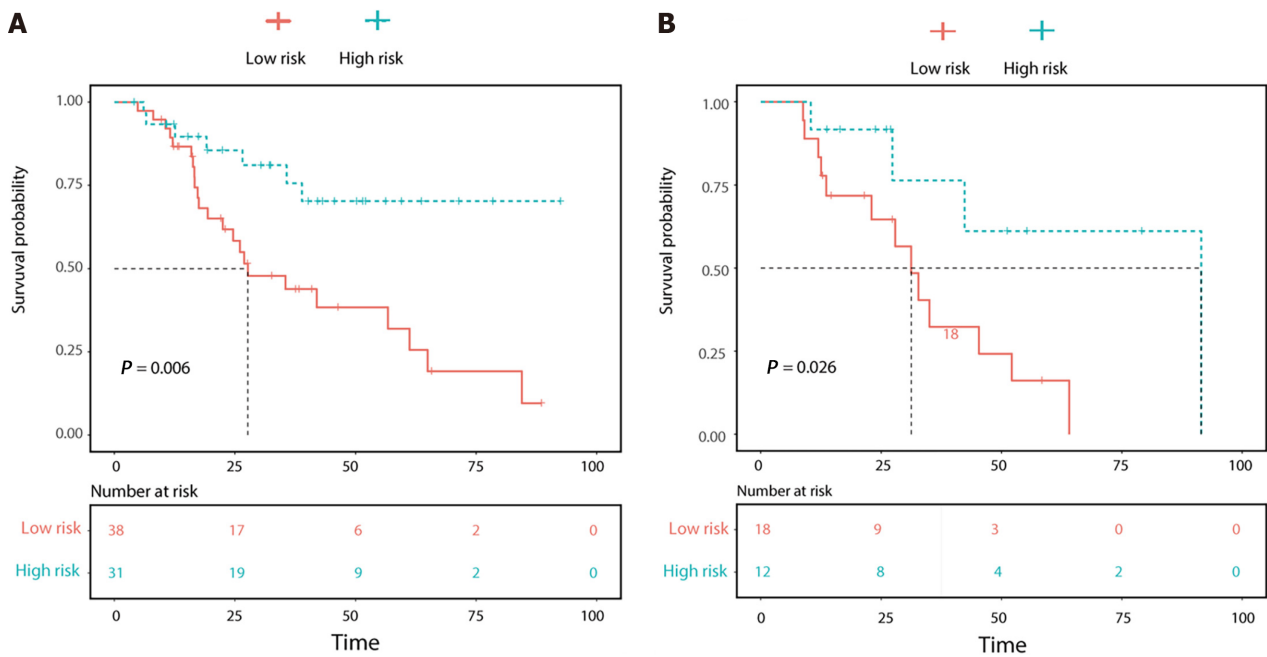


**Figure 5 Overall survival (OS) curve analysis.** A: The OS curve estimates by clinic-radiological-radiomics model in patients with  $\beta$ -Arrestin1 phosphorylation positive and  $\beta$ -Arrestin1 phosphorylation negative in the training cohort; B: The OS curve estimates by clinic-radiological-radiomics model in patients with  $\beta$ -Arrestin1 phosphorylation positive and  $\beta$ -Arrestin1 phosphorylation negative in the validation cohort.

The clinicopathologic features of preoperative serum ALT levels were significantly different in the p- $\beta$ -arrestin1-positive and p- $\beta$ -arrestin1-negative groups in this study. In line with the findings of previous studies, serum ALT is an important hepatic inflammation marker that is correlated with liver function. Hepatitis infection can simultaneously induce serum ALT increases and  $\beta$ -arrestin1 upregulation, and higher serum ALT levels are a feature commonly associated with this subtype of HCC[12]. In clinical practice, serum ALT levels can be easily obtained and incorporated into a radiomics model for individualized risk estimation. A larger tumor size and nonsmooth tumor margins were also shown to be associated with p- $\beta$ -arrestin1 expression. This finding is in accordance with previous studies showing that  $\beta$ -arrestin1 can promote hepatocellular proliferation *via* the Akt pathway, and HCCs with higher p- $\beta$ -arrestin1 levels are more likely to have an infiltrative growth pattern[13]. Serum AST levels were associated with p- $\beta$ -arrestin1 in the univariate analysis but not the multivariate models, probably because of a lack of statistical power due to the insufficient number of patients.

We also found that patients who were p- $\beta$ -arrestin1-positive lived longer than those who were p- $\beta$ -arrestin1-negative. Previous studies have revealed that high expression of  $\beta$ -arrestin1 contributes to tumor survival, proliferation, angiogenesis, invasion and metastasis and is associated with the prognosis of epithelial ovarian cancer, prostate cancer and lung cancer[30-34]. Although the correlation of  $\beta$ -arrestin1 with HCC prognosis has not been investigated,  $\beta$ -arrestin1 has been shown to be positively related to HCC carcinogenesis and metastasis[12,13]. Evidence has shown that the sorafenib response is impaired in HCC with dysregulated phosphorylated ERK (p-ERK) and AKT (p-AKT) activation and that suppression of ERK1/2 increases sorafenib sensitivity in several HCC cell lines[35-37], while  $\beta$ -arrestin1 can activate PI3K/Akt signaling by Akt phosphorylation and trigger ERK1/2 phosphorylation-mediated EMT in HCC. Moreover, hyperactive PI3K/AKT signaling has been reported to be one of the primary causes of EMT in HCC resistance to sorafenib[35,36,38]. These studies indicate that PI3K/AKT signaling and p-ERK1/2-mediated EMT signal hyperactivity may function in  $\beta$ -arrestin1-induced HCC resistance to sorafenib and further influence the prognosis of HCC patients treated with sorafenib, which was consistent with a series of studies recently showing that  $\beta$ -arrestin1 expression had some correlation with resistance to therapy in several types of cancers, such as breast[39] ovarian[40,41] and non-small-cell lung cancer[42]. Increased phosphorylation of  $\beta$ -arrestin1 leads to decreased levels of dephosphorylated  $\beta$ -arrestin1, which influences its function in the activation of downstream factors, such as p-ERK and p-AKT. Therefore, the phosphorylation status of  $\beta$ -arrestin1 has a critical role in HCC sorafenib resistance. Predicting p- $\beta$ -arrestin1 can help to identify patients who are sensitive to this treatment and prevent unnecessary side effects.

There were some limitations in our study. First, this was a retrospective longitudinal cohort study and selection bias may exist due to the strict inclusion criteria. Although we performed internal validation, additional external validation is needed to facilitate the wider use of this predictive model. Second, our study was performed at a single institution, and the CT scanner in this study was not fixed in their protocol. However, this could be a strength in terms of the generalizability of the findings by reflecting actual clinical practice. Third, p- $\beta$ -arrestin1 positivity was defined as a cutoff of 5% for tumor

cells to avoid false-positive results. The association between our predictive model and the graded degree of p- $\beta$ -arrestin1 immunopositivity should be further assessed.

---

## CONCLUSION

---

In conclusion, CECT-based radiomics combining clinico-radiological factors achieved desirable results in the prediction of  $\beta$ -arrestin1 phosphorylation in HCC which showed prognostic value in patients treated with sorafenib. This finding suggests that CT radiomics may provide promising and noninvasive biomarkers for the evaluation of p- $\beta$ -arrestin1 expression and may help identify the subset of HCC patients who are more sensitive to sorafenib treatment, thus potentially guiding personalized treatment strategies.

## ARTICLE HIGHLIGHTS

### **Research background**

Sorafenib is regarded as a first-line systematic treatment option for patients with advanced hepatocellular carcinoma (HCC), but its efficacy is largely influenced by raising resistance. The phosphorylation status of  $\beta$ -arrestin1 influences its function as a signal strongly related to sorafenib resistance.

### **Research motivation**

Identifying patients who are more likely to benefit from sorafenib treatment and discovering related biomarkers associated with sorafenib treatment response can guide personal management.

### **Research objectives**

The purpose of this study was to develop and validate radiomics-based models for predicting  $\beta$ -arrestin1 phosphorylation in HCC with contrast-enhanced computed tomography (CT).

### **Research methods**

We included ninety-nine HCC patients (training cohort:  $n = 69$ ; validation cohort:  $n = 30$ ) who received systemic sorafenib treatment after surgery. Radiomics features were generated and selected to build a radiomics score and then combined with clinical and imaging features to establish clinico-radiological (CR) and clinico-radiological-radiomics (CRR) models. The performance and clinical usefulness of the models were measured by receiver operating characteristic and decision curves. Their association with prognosis was also evaluated using the Kaplan-Meier method.

### **Research results**

Our study found that the ALT level, tumor size and tumor margin were significant independent factors for predicting  $\beta$ -arrestin1 phosphorylation. The CRR model showed better discriminative performance than the radiomic score or the CR model. The  $\beta$ -arrestin1 phosphorylation status predicted by the CRR model was shown to be significantly associated with overall survival.

### **Research conclusions**

The radiomics signature is a reliable tool for evaluating  $\beta$ -arrestin1 phosphorylation, and may help to better identify patients who would benefit from sorafenib treatment.

### **Research perspectives**

The results of this study suggests that CT-based radiomics may provide promising and noninvasive biomarkers for the evaluation of  $\beta$ -arrestin1 phosphorylation and may help to identify the subset of HCC patients who are more sensitive to sorafenib treatment, thus potentially guiding personalized treatment strategies.

---

## FOOTNOTES

---

**Author contributions:** Che F, Xu Q, Shi YJ and Song B designed the research; Che F, Li Q and Xu Q conducted literature search and analysis; Yang CW, Huang ZX, Wang LY and Wei Y provided material support; Song B provided funding for the article; Che F and Xu Q wrote the paper; Che F and Xu Q contributed equally to this work.

**Supported by** the Science and Technology Support Program of Sichuan Province, No. 2021YFS0144 and No. 2021YFS0021; China Postdoctoral Science Foundation, No. 2021M692289; and National Natural Science Foundation of

China, No. 81971571.

**Institutional review board statement:** This study was approved by the Ethics Committee of West China Hospital.

**Informed consent statement:** Patients were not required to give informed consent to the study because this retrospective study used anonymous clinical data that were obtained after each patient agreed to treatment by written consent.

**Conflict-of-interest statement:** We have no financial relationships to disclose.

**Data sharing statement:** No additional data are available.

**Open-Access:** This article is an open-access article that was selected by an in-house editor and fully peer-reviewed by external reviewers. It is distributed in accordance with the Creative Commons Attribution NonCommercial (CC BY-NC 4.0) license, which permits others to distribute, remix, adapt, build upon this work non-commercially, and license their derivative works on different terms, provided the original work is properly cited and the use is non-commercial. See: <https://creativecommons.org/licenses/by-nc/4.0/>

**Country/Territory of origin:** China

**ORCID number:** Feng Che 0000-0002-8008-2696; Qing Xu 0000-0001-9438-5535; Qian Li 0000-0001-8330-7654; Zi-Xing Huang 0000-0001-7967-5948; Cai-Wei Yang 0000-0003-3335-3948; Li-Ye Wang 0000-0002-5535-4514; Yi Wei 0000-0003-3993-9747; Yu-Jun Shi 0000-0003-0494-6023; Bin Song 0000-0002-7269-2101.

**S-Editor:** Wu YXJ

**L-Editor:** A

**P-Editor:** Yu HG

## REFERENCES

- 1 **Sung H**, Ferlay J, Siegel RL, Laversanne M, Soerjomataram I, Jemal A, Bray F. Global Cancer Statistics 2020: GLOBOCAN Estimates of Incidence and Mortality Worldwide for 36 Cancers in 185 Countries. *CA Cancer J Clin* 2021; **71**: 209-249 [PMID: 33538338 DOI: 10.3322/caac.21660]
- 2 **Llovet JM**, Ricci S, Mazzaferro V, Hilgard P, Gane E, Blanc JF, de Oliveira AC, Santoro A, Raoul JL, Forner A, Schwartz M, Porta C, Zeuzem S, Bolondi L, Gretten TF, Galle PR, Seitz JF, Borbath I, Häussinger D, Giannaris T, Shan M, Moscovici M, Voliotis D, Bruix J; SHARP Investigators Study Group. Sorafenib in advanced hepatocellular carcinoma. *N Engl J Med* 2008; **359**: 378-390 [PMID: 18650514 DOI: 10.1056/NEJMoa0708857]
- 3 **Cheng AL**, Kang YK, Chen Z, Tsao CJ, Qin S, Kim JS, Luo R, Feng J, Ye S, Yang TS, Xu J, Sun Y, Liang H, Liu J, Wang J, Tak WY, Pan H, Burock K, Zou J, Voliotis D, Guan Z. Efficacy and safety of sorafenib in patients in the Asia-Pacific region with advanced hepatocellular carcinoma: a phase III randomised, double-blind, placebo-controlled trial. *Lancet Oncol* 2009; **10**: 25-34 [PMID: 19095497 DOI: 10.1016/S1470-2045(08)70285-7]
- 4 **Lin FT**, Krueger KM, Kendall HE, Daaka Y, Fredericks ZL, Pitcher JA, Lefkowitz RJ. Clathrin-mediated endocytosis of the beta-adrenergic receptor is regulated by phosphorylation/dephosphorylation of beta-arrestin1. *J Biol Chem* 1997; **272**: 31051-31057 [PMID: 9388255 DOI: 10.1074/jbc.272.49.31051]
- 5 **Whalen EJ**, Rajagopal S, Lefkowitz RJ. Therapeutic potential of  $\beta$ -arrestin- and G protein-biased agonists. *Trends Mol Med* 2011; **17**: 126-139 [DOI: 10.1016/j.molmed.2010.11.004]
- 6 **Ezzoukhry Z**, Louandre C, Trécherel E, Godin C, Chauffert B, Dupont S, Diouf M, Barbare JC, Mazière JC, Galmiche A. EGFR activation is a potential determinant of primary resistance of hepatocellular carcinoma cells to sorafenib. *Int J Cancer* 2012; **131**: 2961-2969 [PMID: 22514082 DOI: 10.1002/ijc.27604]
- 7 **Ma Y**, Xu R, Liu X, Zhang Y, Song L, Cai S, Zhou S, Xie Y, Li A, Cao W, Tang X. LY3214996 relieves acquired resistance to sorafenib in hepatocellular carcinoma cells. *Int J Med Sci* 2021; **18**: 1456-1464 [PMID: 33628103 DOI: 10.7150/ijms.51256]
- 8 **Negri FV**, Dal Bello B, Porta C, Campanini N, Rossi S, Tinelli C, Poggi G, Missale G, Fanello S, Salvagni S, Ardizzoni A, Maria SE. Expression of pERK and VEGFR-2 in advanced hepatocellular carcinoma and resistance to sorafenib treatment. *Liver Int* 2015; **35**: 2001-2008 [PMID: 25559745 DOI: 10.1111/liv.12778]
- 9 **Mendoza MC**, Er EE, Blenis J. The Ras-ERK and PI3K-mTOR pathways: cross-talk and compensation. *Trends Biochem Sci* 2011; **36**: 320-328 [PMID: 21531565 DOI: 10.1016/j.tibs.2011.03.006]
- 10 **Zhang PF**, Li KS, Shen YH, Gao PT, Dong ZR, Cai JB, Zhang C, Huang XY, Tian MX, Hu ZQ, Gao DM, Fan J, Ke AW, Shi GM. Galectin-1 induces hepatocellular carcinoma EMT and sorafenib resistance by activating FAK/PI3K/AKT signaling. *Cell Death Dis* 2016; **7**: e2201 [PMID: 27100895 DOI: 10.1038/cddis.2015.324]
- 11 **Chen HA**, Kuo TC, Tseng CF, Ma JT, Yang ST, Yen CJ, Yang CY, Sung SY, Su JL. Angiopoietin-like protein 1 antagonizes MET receptor activity to repress sorafenib resistance and cancer stemness in hepatocellular carcinoma. *Hepatology* 2016; **64**: 1637-1651 [PMID: 27530187 DOI: 10.1002/hep.28773]
- 12 **Yang Y**, Guo Y, Tan S, Ke B, Tao J, Liu H, Jiang J, Chen J, Chen G, Wu B.  $\beta$ -Arrestin1 enhances hepatocellular carcinogenesis through inflammation-mediated Akt signalling. *Nat Commun* 2015; **6**: 7369 [PMID: 26077142 DOI: 10.1038/ncomms8369]

- 13 **Xu X**, Lei Y, Zhou H, Guo Y, Liu H, Jiang J, Yang Y, Wu B.  $\beta$ -Arrestin1 is involved in hepatocellular carcinoma metastasis via extracellular signal-regulated kinase-mediated epithelial-mesenchymal transition. *J Gastroenterol Hepatol* 2020; **35**: 2229-2240 [PMID: 32445259 DOI: 10.1111/jgh.15115]
- 14 **Lin FT**, Miller WE, Luttrell LM, Lefkowitz RJ. Feedback regulation of beta-arrestin1 function by extracellular signal-regulated kinases. *J Biol Chem* 1999; **274**: 15971-15974 [PMID: 10347142 DOI: 10.1074/jbc.274.23.15971]
- 15 **Cohen JV**, Sullivan RJ. Developments in the Space of New MAPK Pathway Inhibitors for BRAF-Mutant Melanoma. *Clin Cancer Res* 2019; **25**: 5735-5742 [PMID: 30992297 DOI: 10.1158/1078-0432.CCR-18-0836]
- 16 **Sun R**, Limkin EJ, Vakalopoulou M, Dercle L, Champiat S, Han SR, Verlingue L, Brandao D, Lancia A, Ammari S, Hollebecque A, Scoazec JY, Marabelle A, Massard C, Soria JC, Robert C, Paragios N, Deutsch E, F ert e C. A radiomics approach to assess tumour-infiltrating CD8 cells and response to anti-PD-1 or anti-PD-L1 immunotherapy: an imaging biomarker, retrospective multicohort study. *Lancet Oncol* 2018; **19**: 1180-1191 [PMID: 30120041 DOI: 10.1016/S1470-2045(18)30413-3]
- 17 **Huang YQ**, Liang CH, He L, Tian J, Liang CS, Chen X, Ma ZL, Liu ZY. Development and Validation of a Radiomics Nomogram for Preoperative Prediction of Lymph Node Metastasis in Colorectal Cancer. *J Clin Oncol* 2016; **34**: 2157-2164 [PMID: 27138577 DOI: 10.1200/JCO.2015.65.9128]
- 18 **Aerts HJ**, Velazquez ER, Leijenaar RT, Parmar C, Grossmann P, Carvalho S, Bussink J, Monshouwer R, Haibe-Kains B, Rietveld D, Hoebers F, Rietbergen MM, Leemans CR, Dekker A, Quackenbush J, Gillies RJ, Lambin P. Decoding tumour phenotype by noninvasive imaging using a quantitative radiomics approach. *Nat Commun* 2014; **5**: 4006 [PMID: 24892406 DOI: 10.1038/ncomms5006]
- 19 **Kickingereder P**, G otz M, Muschelli J, Wick A, Neuberger U, Shinohara RT, Sill M, Nowosielski M, Schlemmer HP, Radbruch A, Wick W, Bendszus M, Maier-Hein KH, Bonekamp D. Large-scale Radiomic Profiling of Recurrent Glioblastoma Identifies an Imaging Predictor for Stratifying Anti-Angiogenic Treatment Response. *Clin Cancer Res* 2016; **22**: 5765-5771 [PMID: 27803067 DOI: 10.1158/1078-0432.CCR-16-0702]
- 20 **Gillies RJ**, Kinahan PE, Hricak H. Radiomics: Images Are More than Pictures, They Are Data. *Radiology* 2016; **278**: 563-577 [PMID: 26579733 DOI: 10.1148/radiol.2015151169]
- 21 **Ma X**, Wei J, Gu D, Zhu Y, Feng B, Liang M, Wang S, Zhao X, Tian J. Preoperative radiomics nomogram for microvascular invasion prediction in hepatocellular carcinoma using contrast-enhanced CT. *Eur Radiol* 2019; **29**: 3595-3605 [PMID: 30770969 DOI: 10.1007/s00330-018-5985-y]
- 22 **Ye Z**, Jiang H, Chen J, Liu X, Wei Y, Xia C, Duan T, Cao L, Zhang Z, Song B. Texture analysis on gadoxetic acid enhanced-MRI for predicting Ki-67 status in hepatocellular carcinoma: A prospective study. *Chin J Cancer Res* 2019; **31**: 806-817 [PMID: 31814684 DOI: 10.21147/j.issn.1000-9604.2019.05.10]
- 23 **Tang C**, Hobbs B, Amer A, Li X, Behrens C, Canales JR, Cuentas EP, Villalobos P, Fried D, Chang JY, Hong DS, Welsh JW, Sepesi B, Court L, Wistuba II, Koay EJ. Development of an Immune-Pathology Informed Radiomics Model for Non-Small Cell Lung Cancer. *Sci Rep* 2018; **8**: 1922 [PMID: 29386574 DOI: 10.1038/s41598-018-20471-5]
- 24 **Xu X**, Zhang HL, Liu QP, Sun SW, Zhang J, Zhu FP, Yang G, Yan X, Zhang YD, Liu XS. Radiomic analysis of contrast-enhanced CT predicts microvascular invasion and outcome in hepatocellular carcinoma. *J Hepatol* 2019; **70**: 1133-1144 [PMID: 30876945 DOI: 10.1016/j.jhep.2019.02.023]
- 25 **Lambin P**, Rios-Velazquez E, Leijenaar R, Carvalho S, van Stiphout RG, Granton P, Zegers CM, Gillies R, Boellard R, Dekker A, Aerts HJ. Radiomics: extracting more information from medical images using advanced feature analysis. *Eur J Cancer* 2012; **48**: 441-446 [PMID: 22257792 DOI: 10.1016/j.ejca.2011.11.036]
- 26 **Segal E**, Sirlin CB, Ooi C, Adler AS, Gollub J, Chen X, Chan BK, Matcuk GR, Barry CT, Chang HY, Kuo MD. Decoding global gene expression programs in liver cancer by noninvasive imaging. *Nat Biotechnol* 2007; **25**: 675-680 [PMID: 17515910 DOI: 10.1038/nbt1306]
- 27 **Hectors SJ**, Lewis S, Besa C, King MJ, Said D, Putra J, Ward S, Higashi T, Thung S, Yao S, Laface I, Schwartz M, Gnjatic S, Merad M, Hoshida Y, Taouli B. MRI radiomics features predict immuno-oncological characteristics of hepatocellular carcinoma. *Eur Radiol* 2020; **30**: 3759-3769 [PMID: 32086577 DOI: 10.1007/s00330-020-06675-2]
- 28 **Wang W**, Gu D, Wei J, Ding Y, Yang L, Zhu K, Luo R, Rao SX, Tian J, Zeng M. A radiomics-based biomarker for cytokeratin 19 status of hepatocellular carcinoma with gadoxetic acid-enhanced MRI. *Eur Radiol* 2020; **30**: 3004-3014 [PMID: 32002645 DOI: 10.1007/s00330-019-06585-y]
- 29 **Forner A**, Llovet JM, Bruix J. Hepatocellular carcinoma. *Lancet* 2012; **379**: 1245-1255 [PMID: 22353262 DOI: 10.1016/S0140-6736(11)61347-0]
- 30 **Shenoy SK**, Han S, Zhao YL, Hara MR, Oliver T, Cao Y, Dewhirst MW.  $\beta$ -arrestin1 mediates metastatic growth of breast cancer cells by facilitating HIF-1-dependent VEGF expression. *Oncogene* 2012; **31**: 282-292 [PMID: 21685944 DOI: 10.1038/onc.2011.238]
- 31 **Zecchini V**, Madhu B, Russell R, P ertega-Gomes N, Warren A, Gaude E, Borlido J, Stark R, Ireland-Zecchini H, Rao R, Scott H, Boren J, Massie C, Asim M, Brindle K, Griffiths J, Frezza C, Neal DE, Mills IG. Nuclear ARRB1 induces pseudohypoxia and cellular metabolism reprogramming in prostate cancer. *EMBO J* 2014; **33**: 1365-1382 [PMID: 24837709 DOI: 10.15252/embj.201386874]
- 32 **Dasgupta P**, Rizwani W, Pillai S, Davis R, Banerjee S, Hug K, Lloyd M, Coppola D, Haura E, Chellappan SP. ARRB1-mediated regulation of E2F target genes in nicotine-induced growth of lung tumors. *J Natl Cancer Inst* 2011; **103**: 317-333 [PMID: 21212384 DOI: 10.1093/jnci/djq541]
- 33 **Wang LG**, Su BH, Du JJ. Expression of  $\beta$ -arrestin 1 in gastric cardiac adenocarcinoma and its relation with progression. *Asian Pac J Cancer Prev* 2012; **13**: 5671-5675 [PMID: 23317236 DOI: 10.7314/apjcp.2012.13.11.5671]
- 34 **Cianfrocca R**, Tocci P, Rosan o L, Caprara V, Sestito R, Di Castro V, Bagnato A. Nuclear  $\beta$ -arrestin1 is a critical cofactor of hypoxia-inducible factor-1 $\alpha$  signaling in endothelin-1-induced ovarian tumor progression. *Oncotarget* 2016; **7**: 17790-17804 [PMID: 26909598 DOI: 10.18632/oncotarget.7461]
- 35 **Huang XY**, Ke AW, Shi GM, Zhang X, Zhang C, Shi YH, Wang XY, Ding ZB, Xiao YS, Yan J, Qiu SJ, Fan J, Zhou J.  $\alpha$  B-crystallin complexes with 14-3-3 $\zeta$  to induce epithelial-mesenchymal transition and resistance to sorafenib in hepatocellular carcinoma. *Hepatology* 2013; **57**: 2235-2247 [PMID: 23316005 DOI: 10.1002/hep.26255]

- 36 **Zhai B**, Sun XY. Mechanisms of resistance to sorafenib and the corresponding strategies in hepatocellular carcinoma. *World J Hepatol* 2013; **5**: 345-352 [PMID: 23898367 DOI: 10.4254/wjh.v5.i7.345]
- 37 **Wang C**, Jin H, Gao D, Liefink C, Evers B, Jin G, Xue Z, Wang L, Beijersbergen RL, Qin W, Bernards R. Phospho-ERK is a biomarker of response to a synthetic lethal drug combination of sorafenib and MEK inhibition in liver cancer. *J Hepatol* 2018; **69**: 1057-1065 [PMID: 30030148 DOI: 10.1016/j.jhep.2018.07.004]
- 38 **van Malenstein H**, Dekervel J, Verslype C, Van Cutsem E, Windmolders P, Nevens F, van Pelt J. Long-term exposure to sorafenib of liver cancer cells induces resistance with epithelial-to-mesenchymal transition, increased invasion and risk of rebound growth. *Cancer Lett* 2013; **329**: 74-83 [PMID: 23111106 DOI: 10.1016/j.canlet.2012.10.021]
- 39 **Lundgren K**, Tobin NP, Lehn S, Stål O, Rydén L, Jirstrom K, Landberg G. Stromal expression of  $\beta$ -arrestin-1 predicts clinical outcome and tamoxifen response in breast cancer. *J Mol Diagn* 2011; **13**: 340-351 [PMID: 21497294 DOI: 10.1016/j.jmoldx.2011.01.009]
- 40 **Rosanò L**, Cianfrocca R, Tocci P, Spinella F, Di Castro V, Caprara V, Semprucci E, Ferrandina G, Natali PG, Bagnato A. Endothelin A receptor/ $\beta$ -arrestin signaling to the Wnt pathway renders ovarian cancer cells resistant to chemotherapy. *Cancer Res* 2014; **74**: 7453-7464. [PMID: 25377471 DOI: 10.1158/0008-5472.CAN-13-3133]
- 41 **Sestito R**, Cianfrocca R, Rosanò L, Tocci P, Di Castro V, Caprara V, Bagnato A. Macitentan blocks endothelin-1 receptor activation required for chemoresistant ovarian cancer cell plasticity and metastasis. *Life Sci* 2016; **159**: 43-48 [PMID: 26776834 DOI: 10.1016/j.lfs.2016.01.009]
- 42 **Jiang Y**, Zhuo X, Fu X, Wu Y, Mao C. Targeting PAR2 Overcomes Gefitinib Resistance in Non-Small-Cell Lung Cancer Cells Through Inhibition of EGFR Transactivation. *Front Pharmacol* 2021; **12**: 625289 [PMID: 33967759 DOI: 10.3389/fphar.2021.625289]



Published by **Baishideng Publishing Group Inc**  
7041 Koll Center Parkway, Suite 160, Pleasanton, CA 94566, USA  
**Telephone:** +1-925-3991568  
**E-mail:** [bpgoffice@wjgnet.com](mailto:bpgoffice@wjgnet.com)  
**Help Desk:** <https://www.f6publishing.com/helpdesk>  
<https://www.wjgnet.com>

